Luminescent Nanoparticles

Deutsche Ausgabe: DOI: 10.1002/ange.201602787
Internationale Ausgabe: DOI: 10.1002/anie.201602787

# Large-Scale Synthesis of Highly Luminescent Perovskite-Related $CsPb_2Br_5$ Nanoplatelets and Their Fast Anion Exchange

*Kun-Hua Wang, Liang Wu, Lei Li, Hong-Bin Yao,* Hai-Sheng Qian, and Shu-Hong Yu**

***Abstract:*** *All-inorganic cesium lead-halide perovskite nanocrystals have emerged as attractive optoelectronic nanomaterials owing to their stabilities and highly efficient photoluminescence. Herein we report a new type of highly luminescent perovskite-related $CsPb_2Br_5$ nanoplatelets synthesized by a facile precipitation reaction. The layered crystal structure of $CsPb_2Br_5$ promoted an anisotropic two-dimensional (2D) crystal growth during the precipitation process, thus enabling the large-scale synthesis of $CsPb_2Br_5$ nanoplatelets. Fast anion exchange has also been demonstrated in as-synthesized $CsPb_2Br_5$ nanoplatelets to extend their photoluminescence spectra to the entire visible spectral region. The large-scale synthesis and optical tunability of $CsPb_2Br_5$ nanoplatelets will be advantageous in future applications of optoelectronic devices.*

Colloidal quasi-2D semiconductor nanoplatelets are an interesting class of nanocrystals owing to their unique photo-physical properties, such as increased exciton binding energy, reduced florescence decay times, and notable optical nonlinearities.[1] Recently, metal halides with perovskite or perovskite-related crystal structures have emerged as attractive semiconducting materials owing to their optoelectronic properties enabling high conversion efficiency in photovoltaics and light-emitting diode devices.[2] Colloidal nanoplatelets of perovskite metal halides are an important class of nanomaterials because they not only enrich the diversity of semiconducting nanomaterials but also potentially provide a platform for exploring new photo-physical properties of 2D semiconducting materials.

Arisen from the high performance of organometal halides recently demonstrated in solar cells, the synthesis and properties of colloidal nanoplatelets of organometal halide hybrid perovskite attracted much attention.[3] The quantum size effect in colloidal organometal halide perovskite nanoplatelets have been explored based on the thickness tuning by surfactant concentration.[3c] Extremely, the atomically thin 2D organic–inorganic hybrid perovskites have been produced via a delicate ternary co-solvent controlled precipitation.[3d] However, the material stability of organometal halide perovskites is becoming a limiting factor for its study and application.[4] All-inorganic perovskite nanocrystals, in which cesium ions replace organic cations, are considered as alternatives to hybrid perovskites owing to their higher stability and extended application range.[5] Very recently, colloidal cesium lead-halide perovskites nanoplatelets have been prepared by the reaction of $PbBr_2$ with metal–organic complex (cesium oleate) in octadecene at relatively high temperature,[6] which is similar to the synthesis of traditional metal chalcogenide nanoparticles.[7] To further explore these new 2D semiconductor materials, other phases of cesium lead-halide nanoplatelets and their large-scale synthesis are in demand, also as an alternative to the limited-scale synthesis of the traditional metal–organic complex decomposition method.[6,8]

Herein, we report a facile fast precipitation synthesis of highly luminescent perovskite-related $CsPb_2Br_5$ nanoplatelets and their fast anion-exchange capabilities to tune optical properties. The colloidal synthesis of $CsPb_2Br_5$ nanoplatelets was carried out by modifying the synthesis of organometal halide perovskite nanoplatelets reported by Sichert et al.,[3c] in which they used a high concentration of octylammonium in the precipitation process to stabilize the quasi-2D methylammonium (MA) lead bromide nanoplatelets. In our study, we found that by using inorganic cations $Cs^+$ to replace organic MA, a comparatively smaller amount of surfactant hexylammonium (HA) with a shorter carbon chain can introduce the formation of $CsPb_2Br_5$ nanoplatelets. This is because the anisotropic 2D growth of $CsPb_2Br_5$ during the precipitation reaction is determined by the intrinsic symmetry of its crystal structure. As shown in Figure 1 a, the tetragonal phase of $CsPb_2Br_5$ exhibits a sandwich structure consisting of $[Pb_2Br_5]^-$ layers and intercalated $Cs^+$. In the $[Pb_2Br_5]^-$ layer (Figure S1 a, in the Supporting Information), one $Pb^{2+}$ coordinates with four $Br^-$ forming the elongated pentahedron. All the $Pb^{2+}$ ions are confined in the center of the layer and both bottom and top surface of the layer are $Br^-$ ions (Figure S1 b). The features of the $CsPb_2Br_5$ crystal structure are similar to that of layered double hydroxides, the nanoplatelets of which have been easily prepared by the facile precipitation process.[9] In contrast, the monoclinic or cubic phase of $CsPbBr_3$ presents a three-dimensional connected structure, in which the octahedral coordination of $Pb^{2+}$ with six $Br^-$ extends to three dimensions via sharing the vertex and $Cs^+$ ions localize in the octahedral voids (Figure 1 b). The

[*] K.-H. Wang, L. Wu, L. Li, Prof. Dr. H. B. Yao, Prof. Dr. S. H. Yu
Division of Nanomaterials & Chemistry, Hefei National Laboratory for Physical Sciences at Microscale, Collaborative Innovation Center of Suzhou Nano Science and Technology, Department of Chemistry
University of Science and Technology of China
Hefei, Anhui 230026 (P.R. China)
E-mail: yhb@ustc.edu.cn
shyu@ustc.edu.cn
Homepage: http://staff.ustc.edu.cn/~yulab/
Prof. Dr. H. S. Qian
School of Medical Engineering, Hefei University of Technology
Hefei, 230009 (China)
Supporting information and the ORCID identification number(s) for the author(s) of this article can be found under http://dx.doi.org/10.1002/anie.201602787.

  

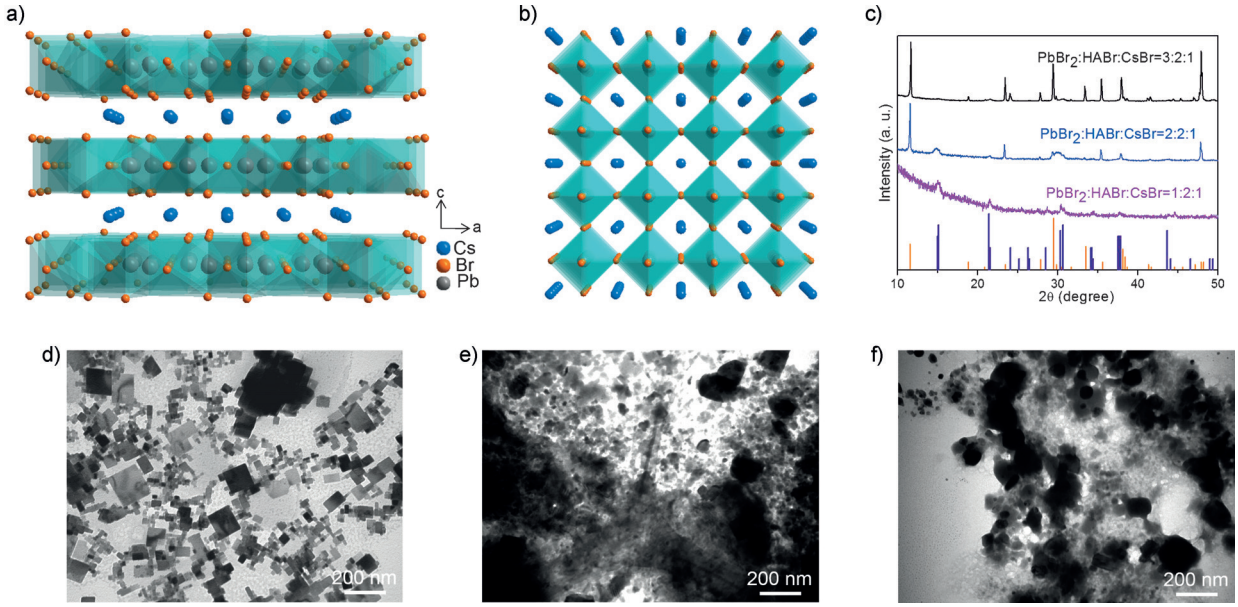


***Figure 1.*** a) Perovskite-related crystal structure of $CsPb_2Br_5$. b) Perovskite crystal structure of $CsPbBr_3$. c) PXRD patterns of the products prepared by the different ratio of reaction precursors. Stick patterns: Standard PXRD of $CsPb_2Br_5$ (PDF#25-0211, orange lines) and $CsPbBr_3$ (PDF#18-0364, violet lines). d)–f) TEM images of the products of different ratio of reaction precursors of $PbBr_2$:HABr:CsBr = 3:2:1, 2:2:1, and 1:2:1, respectively.

difference in the intrinsic symmetry of the crystal structures of $CsPb_2Br_5$ and $CsPbBr_3$ determined their different crystal growth behavior in precipitation reactions.

In a typical synthesis, 10 mL of a dimethylformamide (DMF) solution containing $PbBr_2$ (0.05 M) and HABr (0.033 M) were added dropwise into 100 mL of toluene forming a mixture, and then 5 mL of CsBr/DMF suspension (0.033 M) was added dropwise into the as-prepared toluene mixture under vigorous stirring. The final molar ratio of $PbBr_2$:HABr:CsBr in the toluene is 3:2:1. The powder X-ray diffraction (PXRD) patterns (Figure 1c, black curve) demonstrated that high crystalline and pure phase of tetragonal $CsPb_2Br_5$ (PDF#25-0211) was synthesized in this fast precipitation reaction. When decreasing the molar ratio of $PbBr_2$:CsBr to 2:1 or 1:1, we found that the monoclinic $CsPbBr_3$ (PDF#18-0364) gradually dominates the precipitation product (Figure 1c blue curve and pink curve), which is consistent with the elemental ratio in the reaction precursor. But the peak intensity of the PXRD pattern of $CsPbBr_3$ is much lower than that of $CsPb_2Br_5$ which indicates that the crystallinity of $CsPbBr_3$ is much lower than that of $CsPb_2Br_5$. This also means that the quasi-2D anisotropic growth of $CsPb_2Br_5$ is much more favorable than that of $CsPbBr_3$ in the precipitation reaction system at room temperature. Transmission electron microscope (TEM) images further confirmed the hypothesis of quasi-2D anisotropic crystal growth derived from the comparison of PXRD patterns. As shown in Figure 1d, the particles in the reaction of $PbBr_2$:HABr:CsBr ratio of 3:2:1 are most square or rectangular nanoplatelets. The statistic size distribution (in *ab* plane) of as-synthesized $CsPb_2Br_5$ nanoplatelets based on the TEM image is summarized in Figure S2 showing that the size of most nanoplatelets (70%) is in the range of around 10–100 nm. The thickness of as-synthesized $CsPb_2Br_5$ nanoplatelets was measured by atomic force microscope (AFM) as approximately 3 nm and nanoplatelets are likely to stack with each other forming the aggregation (Figure S3). In contrast, with decreasing the molar ratio of $PbBr_2$:CsBr to 2:1 in the solution, the morphologies of generated $CsPb_2Br_5$ nanoplatelets were not well-defined square or rectangular and many irregular nanoparticles appeared due to the precipitation of $CsPbBr_3$ (Figure 1e). When the ratio of $PbBr_2$:CsBr is 1:1 in the solution, the nanoplatelets of $CsPb_2Br_5$ totally disappeared and random sizes of nanoparticles were yielded (Figure 1f) indicating that the crystal growth of $CsPbBr_3$ is uncontrollable in this solution with relatively low concentration of surfactant (HA).

The synthesis of $CsPb_2Br_5$ nanoplatelets by this facile precipitation process is easy to be scaled up (see Experimental Section, Supporting Information). All the precipitation process can be completed in several minutes (Movie S1) indicating the feasibility of the generation of $CsPb_2Br_5$ nanoplatelets. The obtained colloidal $CsPb_2Br_5$ nanoplatelets suspension was shown in Figure 2a and it emitted green light under the UV light (365 nm) irradiation (Figure 2b). The finally obtained yellow $CsPb_2Br_5$ nanoplatelets powder produced by a one-pot reaction was weighted as approximately 0.5 g (Figure S4a) and still maintained highly photoluminescence with emitting green light under the UV light (365 nm) irradiation (Figure S4b). The phase of the product synthesized in large scale is the pure tetragonal $CsPb_2Br_5$ (Figure 2c). UV/Vis adsorption and photoluminescence emission spectra of as-obtained colloidal $CsPb_2Br_5$ nanoplatelets are presented in Figure 2d. The absorption spectrum is dominated by sharp exciton peaks which is similar to the optical features of previously reported $CsPbBr_3$[6] and CdSe[1a] nano-

  

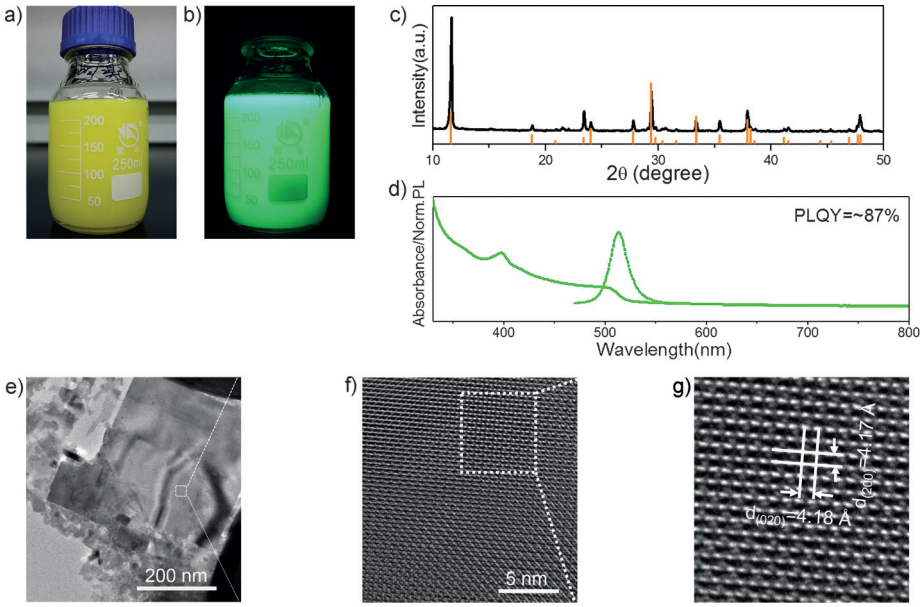


***Figure 2.*** a),b) Photographs of as-obtained colloidal $CsPb_2Br_5$ nanoplatelets suspension under ambient conditions and the UV light (365 nm) irradiation, respectively. c) PXRD of the product synthesized in a relatively large scale reaction. Orange lines: standard PXRD of $CsPb_2Br_5$ (PDF#25-0211). d) Absorption (left) and PL (right) spectrum of colloidal $CsPb_2Br_5$ nanoplatelets toluene solution. e)–g) TEM and HRTEM images of $CsPb_2Br_5$ nanoplatelets, respectively.

platelets. The PL emission spectrum of the $CsPb_2Br_5$ exhibited a highly symmetric band centered at 512 nm with narrow 12 nm full-width-at-half-maximum (FWHM). The absolute PL quantum yield (PLQY) of $CsPb_2Br_5$ nanoplatelets in toluene solution is about 87%. TEM image in Figure 2e further displayed that the nanostructures of as-synthesized $CsPb_2Br_5$ are well-defined rectangular platelets. High resolution TEM (HRTEM) clearly shows the two dimensional lattice fringe (Figure 2f). The measured d-spacing values of these two perpendicular lattice fringes were 0.418 nm and 0.417 nm (Figure 2g) corresponding to that of (020) and (200) planes of tetragonal $CsPb_2Br_5$, respectively. This result further illustrated that the lateral 2D anisotropic growth directions of $CsPb_2Br_5$ nanoplatelets is along the *ab* plane.

We adopted different reaction precursors to explore the influence of ions on the precipitation of $CsPb_2X_5$ (X = Cl, Br or I) nanoplatelets. The reaction details are summarized in Table S1–5. When the MABr was used to replace CsBr, the dominate phase in the products is monoclinic $MAPbBr_3$ with a tiny amount of tetragonal $MAPb_2Br_5$ (Figure 3a, pink curve). Using CsCl to replace CsBr resulted in the formation of the pure phase of $CsPb_2Br_{5-x}Cl_x$ (Figure 3a, black curve) but the CsI resulted in the formation of the impurity of $CsPbBr_{3-x}I_x$ (Figure 3a red curve). The replacement of HABr by HACl or HAI exhibited the similar phenomenon that the pure tetragonal phase of $CsPb_2Br_{5-x}Cl_x$ was obtained (Figure 3a blue curve) but the impure phase of $CsPbBr_{3-x}I_x$ appeared in

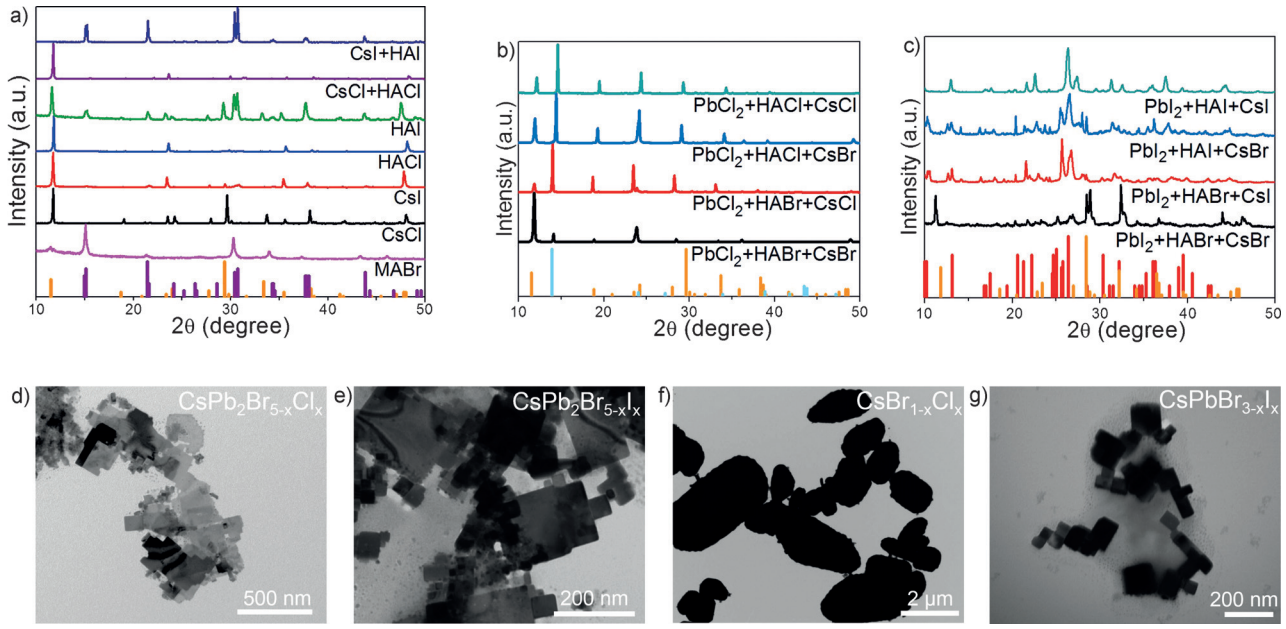


***Figure 3.*** a)–c) PXRD patterns of reaction products by using different reaction precursors (listed) in precipitation systems. Stick patterns: Standard PXRD of $CsPb_2Br_5$ (PDF#25-0211, orange lines), $CsPbBr_3$ (PDF#18-0364, violet lines), CsBr (PDF#52-1144, cyan lines), and $CsPbI_3$ (PDF#18-0376, red lines). d)–g) TEM images showing the representative nanostructures of $CsPb_2Br_{5-x}Cl_x$, $CsPb_2Br_{5-x}I_x$, $CsBr_{1-x}Cl_x$, and $CsPbBr_{3-x}I_x$, respectively.

the reaction (Figure 3a green curve). When the HABr and CsBr were both replaced by the HACl and CsCl the resulted product is pure tetragonal $CsPb_2Br_{5-x}Cl_x$ (Figure 3a violet curve). In contrast, using HAI and CsI leaded to the formation of pure monoclinic $CsPbBr_{3-x}I_x$ (Figure 3a dark blue curve). The above results indicate that $I^-$ with relatively big ionic radius limited the 2D growth of $CsPb_2Br_{5-x}I_x$ but $Cl^-$ shows little influence on the formation of tetragonal phase of $CsPb_2Br_{5-x}Cl_x$. The replacement of lead salt resulted in remarkable variation of the precipitated products without the formation of pure tetragonal phase of $CsPb_2Br_{5-x}Cl_x$ or $CsPb_2Br_{5-x}I_x$. When the $PbCl_2$ was used as the reaction precursor the obtained products contains both the $CsPb_2Br_{5-x}Cl_x$ and $CsBr_{1-x}Cl_x$ (Figure 3b). The $PbI_2$ reaction precursor resulted in the formation of orthorhombic $CsPbI_3$ (Figure 3c). TEM images (Figure 3d–g) further show the different nanostructures of obtained products. As shown in Figure 3d,e, $CsPb_2Br_{5-x}Cl_x$ or $CsPb_2Br_{5-x}I_x$ present typical 2D platelet-like structures. In contrast, the morphologies of $CsBr_{1-x}Cl_x$ and $CsPbI_3$ are random microparticles and brick-like nanoparticles, respectively (Figure 3f,g), which indicate the uncontrolled crystal growth of $CsBr_{1-x}Cl_x$ and $CsPbI_3$ in the reaction system.

Ion exchange is a versatile tool for nanomaterial synthesis, which has been used to prepare various nanostructured materials.[10] In our case, as-prepared highly photoluminescent $CsPb_2Br_5$ nanoplatelets exhibited fast anion exchange behavior similar to very recently reported $CsPbBr_3$ cubic nanocrystals.[11] The anion-exchange reactions in our case were conducted in toluene as a solvent by mixing a specific ration of the desired halide source (HACl or HAI) and $CsPb_2Br_5$ nanoplatelets (see Experimental Section and Table S6, Supporting Information). This anion exchange process can be achieved in tens of seconds (Movie S2) at room temperature indicating the fast diffusion capability of halide ions in these $CsPb_2X_5$ nanoplatelets. As shown in Figure S5, through the gradual anion exchange from Br-to-Cl, the color of the $CsPb_2Br_5$ nanoplatelets suspension changed from yellow to light green and then to green-white. In the case of anion exchange from Br-to-I, the color of the suspension changed from yellow to orange and then to red. The energy dispersive spectroscopy (EDS) analysis (Figure S6–7 and Table S7) also indicates that the exchanged anions in final nanoplatelets increased with the increase of the amount of halide sources added into the solution. To show the tunable optical properties realized by anion exchange, the anion-exchanged samples were characterized by the UV/Vis adsorption and photoluminescence spectroscopy. As shown in Figure 4a, the anion exchange reactions led to a blue shift

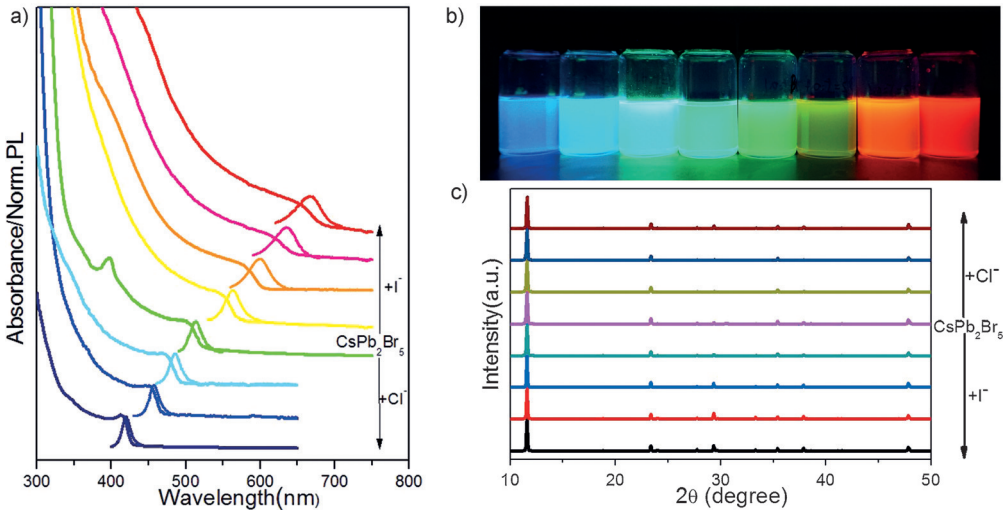


***Figure 4.*** a) Evolution of the optical absorption (left) and PL (right) spectra of $CsPb_2Br_5$ nanoplatelets with increasing quantities of anion-exchange of $I^-$ and $Cl^-$, respectively. b) Photograph of $CsPb_2Br_5$ nanoplatelets under the irradiation of a 365 nm UV lamp. c) PXRD patterns of the parent $CsPb_2Br_5$ nanoplatelet and anion-exchanged samples.

(for Br-to-Cl) or a red shift (for Br-to-I) of the optical features, correlating with the incorporation of the new anions. photoluminescence of the obtained nanoplatelets can cover all visible spectra and exhibited the bright and narrow emission from blue to red. The photograph of the entire visible spectrum emission of anion-exchanged samples under UV light (365 nm) irradiation is shown in Figure 4b. The PLQY of the obtained nanoplatelets are in the range of approximately 20–90% (Figure S8), which is comparable to that of previously synthesized $CsPbX_3$ cubic nanocrystals.[8b] Notably, with further processing the anion exchange the PLQY of nanoplatelets decreased to a lower value with respect to original $CsPb_2Br_5$, which is ascribed to intrinsic properties of halide perovskites.[12]

The phases of anion-exchanged samples were analyzed by PXRD (Figure 4c) indicating that the anion exchange process did not deteriorate the layered crystal structure feature and remarkably alter the crystal lattice. The details of PXRD peaks at low angle (Figure S9) further showed that upon incorporation of $Cl^-$, the distance between $Pb_2X_5^-$ layers shrunk, while the incorporation of $I^-$, the distance expanded. This also means that upon halides anion exchange the homogenous $CsPb_2Br_{5-x}Cl_x$ or $CsPb_2Br_{5-x}I_x$ solid solutions were formed in the layered structures. In addition, the nanostructures of anion exchanged samples were still maintained as nanoplatelets (Figure S10) and the thickness of the ion exchanged nanoplatelets is approximately 3 nm as well (Figure S11,12) further indicating the stability of the layered structures of $CsPb_2Br_5$ during anion exchange processes.

  

In summary, we report a facile and scalable route for the synthesis of highly luminescent perovskites-related $CsPb_2Br_5$ nanoplatelets. The fast anion-exchange performance of the as-obtained $CsPb_2Br_5$ nanoplatelets has been demonstrated to extend their photoluminescence to the entire visible spectrum. These novel perovskites-related nanoplatelets have potential for application in optoelectronic devices.

## Acknowledgements

This work is supported by the National Natural Science Foundation of China (Grant 51571184, 21431006), the Foundation for Innovative Research Groups of the National Natural Science Foundation of China (Grant 21521001), the National Basic Research Program of China (Grants 2014CB931800, 2013CB931800), the Users with Excellence and Scientific Research Grant of Hefei Science Center of CAS (2015HSC-UE007, 2015SRG-HSC038), and the Chinese Academy of Sciences (Grant KJZD-EW-M01-1).

**Keywords:** anion exchange · cesium lead halides · nanoplatelets · perovskites · photoluminescence

**How to cite:** *Angew. Chem. Int. Ed.* **2016**, *55*, 8328–8332
*Angew. Chem.* **2016**, *128*, 8468–8472

[1] a) S. Ithurria, M. D. Tessier, B. Mahler, R. P. S. M. Lobo, B. Dubertret, A. L. Efros, *Nat. Mater.* **2011**, *10*, 936–941; b) C. E. Rowland, I. Fedin, H. Zhang, S. K. Gray, A. O. Govorov, D. V. Talapin, R. D. Schaller, *Nat. Mater.* **2015**, *14*, 484–489; c) C. Schliehe, B. H. Juarez, M. Pelletier, S. Jander, D. Greshnykh, M. Nagel, A. Meyer, S. Foerster, A. Kornowski, C. Klinke, H. Weller, *Science* **2010**, *329*, 550–553; d) Z. Tang, Z. Zhang, Y. Wang, S. C. Glotzer, N. A. Kotov, *Science* **2006**, *314*, 274–278.

[2] a) Z.-K. Tan, R. S. Moghaddam, M. L. Lai, P. Docampo, R. Higler, F. Deschler, M. Price, A. Sadhanala, L. M. Pazos, D. Credgington, F. Hanusch, T. Bein, H. J. Snaith, R. H. Friend, *Nat. Nanotechnol.* **2014**, *9*, 687–692; b) N. J. Jeon, J. H. Noh, W. S. Yang, Y. C. Kim, S. Ryu, J. Seo, S. I. Seok, *Nature* **2015**, *517*, 476–480; c) M. M. Lee, J. Teuscher, T. Miyasaka, T. N. Murakami, H. J. Snaith, *Science* **2012**, *338*, 643–647; d) A. Mei, X. Li, L. Liu, Z. Ku, T. Liu, Y. Rong, M. Xu, M. Hu, J. Chen, Y. Yang, M. Grätzel, H. Han, *Science* **2014**, *345*, 295–298.

[3] a) Y. Ling, Z. Yuan, Y. Tian, X. Wang, J. C. Wang, Y. Xin, K. Hanson, B. Ma, H. Gao, *Adv. Mater.* **2016**, *28*, 305–311; b) S. Pathak, N. Sakai, F. Wisnivesky Rocca Rivarola, S. D. Stranks, J. Liu, G. E. Eperon, C. Ducati, K. Wojciechowski, J. T. Griffiths, A. A. Haghighirad, A. Pellaroque, R. H. Friend, H. J. Snaith, *Chem. Mater.* **2015**, *27*, 8066–8075; c) J. A. Sichert, Y. Tong, N. Mutz, M. Vollmer, S. Fischer, K. Z. Milowska, R. G. Cortadella, B. Nickel, C. Cardenas-Daw, J. K. Stolarczyk, A. S. Urban, J. Feldmann, *Nano Lett.* **2015**, *15*, 6521–6527; d) L. Dou, A. B. Wong, Y. Yu, M. Lai, N. Kornienko, S. W. Eaton, A. Fu, C. G. Bischak, J. Ma, T. Ding, N. S. Ginsberg, L.-W. Wang, A. P. Alivisatos, P. Yang, *Science* **2015**, *349*, 1518–1521; e) Y. Fu, F. Meng, M. B. Rowley, B. J. Thompson, M. J. Shearer, D. Ma, R. J. Hamers, J. C. Wright, S. Jin, *J. Am. Chem. Soc.* **2015**, *137*, 5810–5818; f) S. Zhuo, J. Zhang, Y. Shi, Y. Huang, B. Zhang, *Angew. Chem. Int. Ed.* **2015**, *54*, 5693–5696; *Angew. Chem.* **2015**, *127*, 5785–5788.

[4] M. Kulbak, D. Cahen, G. Hodes, *J. Phys. Chem. Lett.* **2015**, *6*, 2452–2456.

[5] J. Song, J. Li, X. Li, L. Xu, Y. Dong, H. Zeng, *Adv. Mater.* **2015**, *27*, 7162–7167.

[6] Y. Bekenstein, B. A. Koscher, S. W. Eaton, P. Yang, A. P. Alivisatos, *J. Am. Chem. Soc.* **2015**, *137*, 16008–16011.

[7] a) L. Wu, B. Quan, Y. Liu, R. Song, Z. Tang, *ACS Nano* **2011**, *5*, 2224–2230; b) W. Han, L. Yi, N. Zhao, A. Tang, M. Gao, Z. Tang, *J. Am. Chem. Soc.* **2008**, *130*, 13152–13161.

[8] a) D. Zhang, S. W. Eaton, Y. Yu, L. Dou, P. Yang, *J. Am. Chem. Soc.* **2015**, *137*, 9230–9233; b) L. Protesescu, S. Yakunin, M. I. Bodnarchuk, F. Krieg, R. Caputo, C. H. Hendon, R. X. Yang, A. Walsh, M. V. Kovalenko, *Nano Lett.* **2015**, *15*, 3692–3696.

[9] a) R. Ma, Z. Liu, K. Takada, N. Iyi, Y. Bando, T. Sasaki, *J. Am. Chem. Soc.* **2007**, *129*, 5257–5263; b) G. G. C. Arizaga, K. G. Satyanarayana, F. Wypych, *Solid State Ionics* **2007**, *178*, 1143–1162.

[10] a) X. Wu, Y. Yu, Y. Liu, Y. Xu, C. Liu, B. Zhang, *Angew. Chem. Int. Ed.* **2012**, *51*, 3211–3215; *Angew. Chem.* **2012**, *124*, 3265–3269; b) Y. Yu, J. Zhang, X. Wu, W. Zhao, B. Zhang, *Angew. Chem. Int. Ed.* **2012**, *51*, 897–900; *Angew. Chem.* **2012**, *124*, 921–924; c) B. J. Beberwyck, Y. Surendranath, A. P. Alivisatos, *J. Phys. Chem. C* **2013**, *117*, 19759–19770; d) D. H. Son, S. M. Hughes, Y. Yin, A. P. Alivisatos, *Science* **2004**, *306*, 1009–1012.

[11] a) Q. A. Akkerman, V. D'Innocenzo, S. Accornero, A. Scarpellini, A. Petrozza, M. Prato, L. Manna, *J. Am. Chem. Soc.* **2015**, *137*, 10276–10281; b) G. Nedelcu, L. Protesescu, S. Yakunin, M. I. Bodnarchuk, M. J. Grotevent, M. V. Kovalenko, *Nano Lett.* **2015**, *15*, 5635–5640.

[12] a) N. Pellet, J. Teuscher, J. Maier, M. Grätzel, *Chem. Mater.* **2015**, *27*, 2181–2188; b) G. Xing, N. Mathews, S. S. Lim, N. Yantara, X. Liu, D. Sabba, M. Grätzel, S. Mhaisalkar, T. C. Sum, *Nat. Mater.* **2014**, *13*, 476–480.

Received: March 22, 2016
Published online: May 23, 2016

  